Effects of Compressibility on Design of Subsonic Fuselages for Natural Laminar Flow

P. M. H. W. Vijgen*
University of Kansas, Lawrence, Kansas
S. S. Dodbele†
Vigyan Research Associates, Inc., Hampton, Virginia
B. J. Holmes‡
NASA Langley Research Center, Hampton, Virginia
and
C. P. van Dam§
University of California, Davis, Davis, California

At high subsonic speeds, density gradients in compressible laminar boundary layers provide increased damping of the two-dimensional and axisymmetric Tollmien-Schlichting instability waves. The favorable influence of flow compressibility provides a unique opportunity to attain natural laminar flow over portions of high-speed subsonic fuselages for drag-reduction purposes. For bodies of moderate fineness ratios (e.g., 5 to 9), the generally destabilizing effect of increasing length-Reynolds number on laminar stability is overpowered by the damping effect of compressibility. Compressible linear stability analyses (based on the e^n method) are presented for the laminar boundary layer on axisymmetric body shapes for length-Reynolds numbers up to 86.6 million and Mach numbers up to 0.80. At a fixed Reynolds number, based on body length, it is predicted that the transition-length Reynolds number triples as the Mach number increases from near zero to 0.80. The favorable effects of flow compressibility on laminar stability might be exploited in the design of external fuel tanks, engine nacelles, and fuselages of business or commuter transports. Attainment of natural laminar flow on the forebodies of larger transport fuselages could provide significant reductions in total drag of transport aircraft.

Nomenclature

A/A_o = ratio of local disturbance amplitude to amplitude at point of neutral stability for fixed disturbance frequency
C_D = body drag coefficient (based on frontal area)
$C_{D_{ref}}$ = drag coefficient for boundary-layer transition location fixed at $x/L = 0.05$ at given Mach number
C_p = pressure coefficient
C_p^* = critical pressure coefficient
F_R = body fineness ratio (body length/maximum body diameter)
L = body length, ft
M = local surface Mach number
M_∞ = freestream Mach number
n = logarithmic exponent of amplitude-growth ratio of unstable Tollmien-Schlichting wave, $n = \ln(A/A_o)$
R_L = Reynolds number based on freestream conditions and body length
R_{TR} = Reynolds number based on freestream conditions and transition length
T.S. = Tollmien-Schlichting
x = axial coordinate starting at nose, ft
x_{TR} = axial location of transition, ft
z = local radius of axisymmetric body, ft
α = angle of attack, deg
ψ = angle of disturbance with respect to streamline, deg

Presented as Paper 86-1825 at the AIAA 4th Applied Aerodynamics Conference, San Diego, CA, June 9-11, 1986; received Oct. 14, 1986; revision received March 8, 1988.

*Research Associate, Flight Research Laboratory; currently at High Technology Corporation, Hampton, VA. Member AIAA.
†Research Scientist. Senior Member AIAA.
‡Head, Flight Applications Branch. Senior Member AIAA.
§Assistant Professor, Department of Mechanical Engineering, Division of Aeronautical Science and Engineering. Member AIAA.

Introduction

EXCEPT for underwater bodies and a few sailplane fuselages, virtually all applied laminar flow research has been focused on airplane lifting surfaces, especially wings. Virtually no research has been conducted on the application of laminar-flow drag-reduction technology to business and transport-airplane fuselages. In the past, the production quality of airframe surfaces was insufficient to permit laminar flow to persist over substantial lengths. Surface roughness typically took the form of unacceptable steps and gaps at skin panel joints. On modern aircraft, however, wing surfaces can be manufactured to meet roughness and waviness criteria for laminar flow.[1,2] As the use of laminar flow on airplane lifting surfaces becomes more widespread, the benefits of achieving laminar flow on other aircraft wetted surfaces, such as the fuselage, will become increasingly attractive. Several aerodynamic and practical issues remain to be resolved before practical engineering design guidance can be offered for laminarization by shaping alone of fuselages and other nonlifting airframe components, such as nacelles of ducted and unducted high-bypass-ratio turbofans and external fuel tanks. The aerodynamic issues include the effects of nonaxisymmetric fuselage shapes on laminar boundary-layer stability (i.e., presence and severity of crossflow in the boundary layer) and the significance of the effects of flow compressibility on the stability of laminar flow over fuselages. Practical concerns for natural laminar flow (NLF) over bodies include the effects of three-dimensional boundary-layer flow on allowable manufacturing tolerances for laminar fuselages

(steps, gaps, and waviness), and the significance of insect contamination on laminar fuselage noses. To date, very few experimental results are available for allowable NLF-surface tolerances over body geometries; Ref. 3 presents limited transition experiments conducted in the 1950's for two- and three-dimensional surface disturbances in the highly accelerating flowfield over a hemisphere. Until new tolerance measurements and transition correlations are available for fuselage geometries, it is believed that, in the absence of significant boundary-layer crossflow, the manufacturing tolerances and waviness requirements for NLF wings[2] apply also to fuselages.

This paper presents the results of a computational analysis of compressible laminar boundary-layer stability on axisymmetric body shapes at Reynolds numbers representative of business and commuter airplanes (i.e., $R_L = 40 \times 10^6$). Potential drag-reduction benefits of attaining NLF on the forward portion of the fuselage of a transport airplane are also discussed.

Background

Most of the past research on the shaping of three-dimensional bodies for laminar flow has been focused on improving performance of submerged bodies in incompressible flow conditions; very limited results have been reported on the viscous-drag reduction of aircraft fuselages. In experimental investigations, Althaus[4] and Radespiel[5] have achieved significant reductions in viscous drag by modifying the body shape of sailplane fuselages. Hertel[6,7] studied the body shapes of fast and prolonged-cruising aquatic animals such as the tuna, shark, and dolphin to gain insight into the possibility of using their body shapes to derive laminar-flow, low-drag transport fuselage shapes. Unfortunately, there are no conclusive experimental data to date establishing the actual state of the boundary layer over these biological shapes at body-length Reynolds numbers of interest for airplane fuselages. Also, Hertel based his innovative extrapolation from fish-body shapes to transport fuselage shapes on integral boundary-layer transition criteria, which have been found to be unreliable for axisymmetric body shapes at higher length-Reynolds numbers.[8] The drag-reduction potential of laminar hydrodynamic bodies was recognized earlier by Carmichael,[9,10] who designed low fineness-ratio axisymmetric bodies that were successfully tested underwater, achieving transition-length Reynolds numbers as high as 18×10^6 at $R_L = 38 \times 10^6$.[11] These promising experimental results paved the way for numerical optimization studies by Parsons et al.,[12] Dalton and Zedan,[13] Pinebrook and Dalton,[14] and Dodbele et al.[8,15] All of these studies investigated the effect of body shape on the viscous drag of axisymmetric bodies for incompressible flow conditions. During the decades since the wind-tunnel and flight experiments by Boltz et al.[16] and Groth,[17] no theoretical or experimental work has been published to investigate the application of natural laminar flow to subsonic fuselages at compressible speeds and relatively high length-Reynolds numbers.

Figure 1 presents the typical drag breakdown for a business-jet and a first-generation long-haul jet transport.[18] As previously noted, the design and production techniques of these older airplanes precluded substantial runs of natural laminar flow over the wing surfaces. Accordingly, for the configurations given in the figure, about half of the total airplane cruise drag originated in skin friction. Figure 2 shows a further breakdown of the total viscous-drag contribution for the transport aircraft, illustrating that, for the all-turbulent transport configuration, the fuselage contributes nearly half of the viscous drag.[19] The achievement of substantial natural laminar flow over the lifting surfaces, as shown on the right of Fig. 2, will increase the relative contribution of the fuselage to the total viscous drag. These figures illustrate the importance of fuselage skin-friction reduction concepts.

A simple analysis is presented herein to illustrate the potential ability to achieve natural laminar flow over a limited length (i.e., the forebody) of a conventional transport fuselage. The resulting drag-reduction benefits appear to be significant and justify further detailed analysis of the possibility to achieve

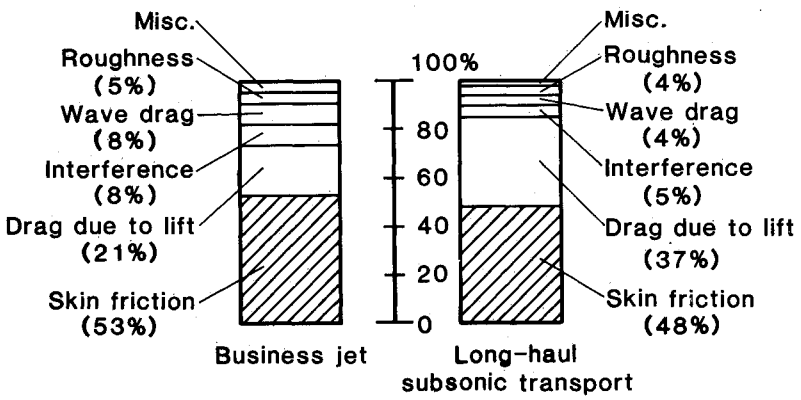

Fig. 1 Total airframe drag breakdown for business-jet and subsonic transport airplane.[18]

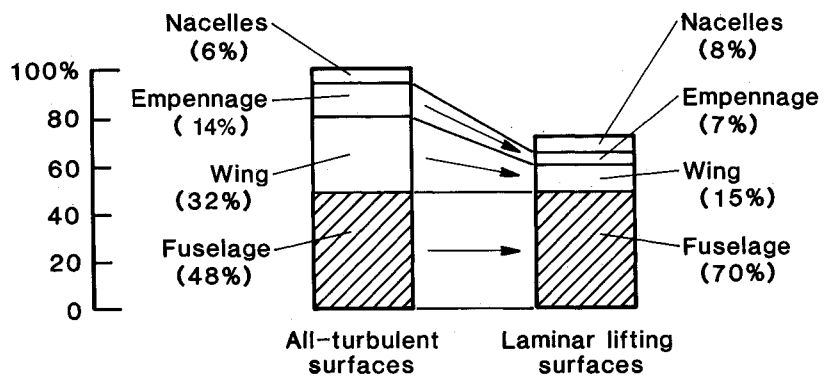

Fig. 2 Viscous-drag breakdown for subsonic transport airplane with and without laminar flow over lifting surfaces.[19]

laminar flow also over nonlifting aircraft surfaces. The measured pressure distribution over a typical transport fuselage at $M_\infty = 0.86$ is shown in Fig. 3.[20] A strong favorable pressure gradient occurs over the forward fuselage section followed by a rapid pressure-recovery gradient. Assuming that the skin-panel joints on the fuselage forebody could be manufactured within laminar-flow tolerances, and that boundary-layer crossflow would not be critical, a transition-length Reynolds number of 30×10^6 would be needed to maintain a laminar boundary layer in the accelerated flow to the end of segment A (at about $x/L = 0.18$) in Fig. 3 at a cruise altitude of 40,000 ft. Maintaining natural laminar flow over segment A is estimated to result in an additional total airplane drag reduction of 6% for a transport airplane having substantial flow over the lifting surfaces (Fig. 2). The combination of both natural laminar flow over segment A and turbulent drag-reduction concepts such as riblets[21] and large-eddy-breakup devices[22] over the remainder of the fuselage could reduce viscous fuselage drag by more than 30%. A 30% reduction in fuselage drag of transports has been estimated to lead to an annual savings in fuel cost of as high as 600 million dollars in 1985 for the U.S. civilian transport fleet. An additional benefit of having a laminar boundary layer over the initial part of the fuselage would be a reduction in turbulent boundary-layer thickness near the end of the fuselage, possibly relieving separation effects, reducing pressure drag, and reducing wing-fuselage juncture interference problems.

The flow acceleration over section A of the transport fuselage is comparable to that which occurs over the forward part of an axisymmetric body with a fineness ratio of approximately 3. Incompressible underwater experiments by Carmichael[11] of unheated bodies with a fineness ratio near 3 have shown transition-length Reynolds numbers as high as 18×10^6. In view of the strongly favorable effect of compressibility on the stability of the two-dimensional laminar boundary layer, as will be discussed in the next section, even larger values of transition-Reynolds numbers could be realized at high-subsonic Mach numbers. Thus, maintaining a laminar boundary layer over the forward part of transport fuselages might become feasible. The effect of a higher cruise altitude on boundary-layer stability is known to be important. At a cruise altitude of 50,000 ft, the unit-Reynolds number is reduced by almost 40% when compared to an altitude of 40,000 ft for constant Mach number; hence, a transition-length Reynolds number of about 20×10^6 would be needed to achieve a laminar boundary layer over the forward transport nose segment. This transition-Reynolds number lies in the range of the experimental observations made by Carmichael.[11]

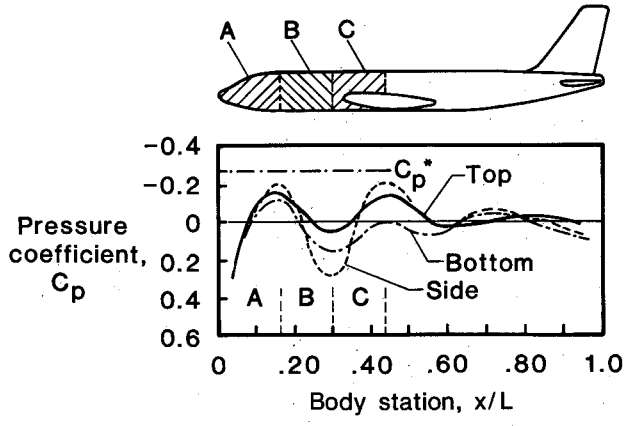

Fig. 3 Measured pressure distribution over fuselage of transport airplane at $M_\infty = 0.86$.[20]

Effects of Compressibility on the Stability of Axisymmetric Subsonic Laminar Boundary Layers

The application of NLF to high-speed, subsonic fuselages could take advantage of the significant influence of compressibility on the stability of two-dimensional and axisymmetric laminar boundary layers. A large amount of recent laminar-flow applications research has been focused on swept wings at high-subsonic speeds corresponding to $M_\infty = 0.60$ to 0.80.[23-25] Wing sweep at higher cruise Mach numbers results in the dominance of three-dimensional (inflectional) crossflow-instability growth in the laminar boundary layer, thereby significantly limiting the extent of NLF attainable over these surfaces. Compressibility hardly influences three-dimensional inflectional instability but can very significantly affect two-dimensional or axisymmetric T.S. instability growth rates.[26] The stability of the laminar boundary layer over axisymmetric fuselages in subsonic cruise flight conditions is dominated by the growth of two-dimensional T.S. disturbances. Thus, compressibility offers a potential for increasing the amount of natural laminar boundary-layer flow over axisymmetric fuselages.

The favorable effects of flow compressibility on axisymmetric boundary-layer stability occur in two ways, one direct and the other indirect. The direct effect results from the development of density gradients in the boundary layer in the direction normal to the surface. For an adiabatic wall, the flow density increases from the wall to the edge of the boundary layer. This effect can provide substantial damping of the two-dimensional viscous T.S. instability waves at freestream Mach numbers below about 2.0.[26-28] The indirect effect results from the influence of compressibility on pressure gradients in the flowfield over aerodynamic bodies. As the subsonic Mach number increases, the pressure gradients become steeper in comparison to the gradients for incompressible flow. Generally, such steepening of favorable pressure gradients increases the stability of the boundary layer against T.S.-type instabilities. Since the flow acceleration that occurs over a three-dimensional body of revolution is relatively small in comparison to a two-dimensional airfoil section of the same profile, the direct effect of density gradients on boundary-layer stability is dominant for bodies with fineness ratios greater than about 5.

Compressible Boundary-Layer Stability Computation

The numerical methods used for the analysis of boundary-layer stability in this paper are described in Ref. 8. For the present application, this computational approach has been modified to include compressibility effects. The pressure distribution over the bodies of revolution at subsonic compressible speeds are predicted by a low-order surface panel method.[29] Local Mach numbers over the geometries considered herein are well below 1.0, permitting the use of a panel method with a compressibility correction. A modified version of the Harris finite-difference, boundary-layer code[30] provides the required boundary-layer velocity and temperature (density) profiles and their smooth derivatives. All boundary-layer calculations in this paper were carried out for adiabatic wall conditions. The finite-difference COSAL code[31] was used to determine the growth of T.S. waves by solving the compressible linear Orr-Sommerfeld eigenvalue problem at each lengthwise station over the axisymmetric body. Obliqueness of the unstable T.S. wave with respect to the streamline direction (ψ) in pure axisymmetric flow does not occur until the local Mach number M exceeds 1.0. Accordingly, in the present analyses of boundary-layer stability over axisymmetric bodies at zero incidence, $\psi = 0$ deg is assumed. The location of onset of transition is assessed using the e^n-method, originally introduced by Van Ingen[32] and Smith.[33] In the e^n-method, the exponent n constitutes a logarithmic amplitude ratio of the instability wave at the streamwise location of interest in comparison to the infinitesimal initial disturbance at the location of neutral stability of the same wave. Generally, the onset of the T.S.-type transition at

incompressible conditions has been correlated to a logarithmic amplification factor of 9-11, depending on the level of freestream disturbances present.[34] In flight experiments, larger values of n factors at transition are generally found due to the absence of critically scaled freestream turbulence and noise levels. Recently, Malik[35] correlated the location of transition in the compressible axisymmetric boundary layer over a cone in a low-supersonic flight experiment ($M_\infty = 1.20$ and 1.50) with an n factor of 9 to 11 using the COSAL method.[31] Also, agreement was reported between the theoretical and measured unstable T.S. wave frequencies near the beginning of transition.

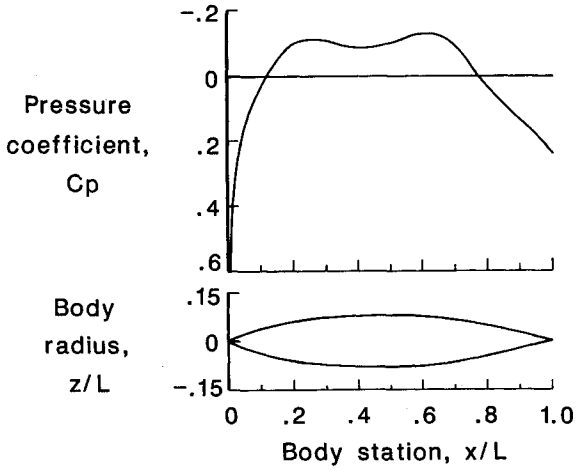

Fig. 4 Geometry and calculated incompressible pressure distribution of body of revolution 6.4-55 ($F_R = 6.4$, maximum body thickness at $x/L = 0.55$); $\alpha = 0$ deg.

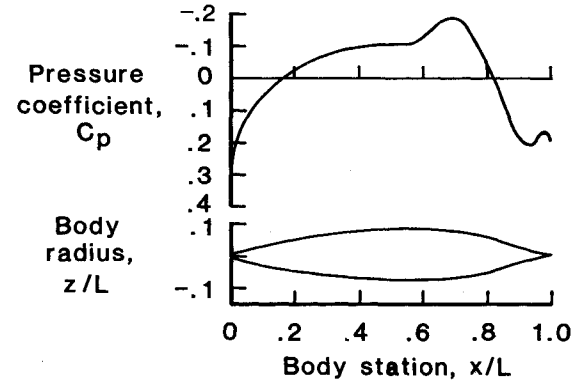

Fig. 5 Geometry and calculated incompressible pressure distribution of body of revolution 6.4-60 ($F_R = 6.4$, maximum body thickness at $x/L = 0.60$); $\alpha = 0$ deg.

This important correlation indicates that T.S. stability analyses based on the e^n-method can also be used as a transition-onset prediction method in compressible conditions, extending the predominantly subsonic incompressible T.S. observations made to date.

Results of Boundary-Layer Stability Calculations

The effects of increasing the freestream Mach number on the pressure distribution for two axisymmetric body shapes are illustrated in Fig. 4 (body designation 6.4-55) and Fig. 5 (body designation 6.4-60). Both of these fuselage shapes are typical of the ones studied in Refs. 8 and 15 for incompressible flow conditions. The body presented in Fig. 4 has its maximum diameter at a location 55% from the nose, and the body in Fig. 5 has the maximum-thickness point at 60%. Both bodies of revolution have a fineness ratio of 6.4.

The incompressible stability characteristics of the two bodies are addressed first to provide a basis for evaluation of the effects of compressibility on boundary-layer stability. Figure 6 shows the results of an incompressible stability analysis[36] for several T.S.-disturbance frequencies for body 6.4-55. Assuming a maximum permissible logarithmic amplification factor of 9, it can be seen from the figure that transition onset is predicted at $x/L = 0.22$ for this geometry at incompressible conditions; i.e., R_{TR} is about 8×10^6. At incompressible conditions, an n-factor of 9 occurs at $x/L = 0.12$ for body 6.4-60 (see Fig. 7). Due to the less steep pressure gradient over its forebody, the geometry of body 6.4-60 is not as conducive to support a laminar boundary layer at incompressible speeds.

The stability characteristics of the laminar boundary layers for both fuselage shapes at compressible conditions are presented next. The 6.4-55 body geometry (Fig. 4) was studied at a Mach number of 0.60 for two different length-Reynolds numbers, while the 6.4-60 body (Fig. 5) was analyzed for freestream Mach numbers of 0.60 and 0.80 at a constant Reynolds number.

Figure 8 presents a comparison of the incompressible and compressible pressure distributions obtained by the panel method over the 6.4-55 body. The predicted development of the unstable T.S. waves in the axial direction ($\psi = 0$ deg) is given in Fig. 9, demonstrating the favorable effect of compressibility on the stability of the laminar boundary layer. Two conclusions may be drawn from the results shown in Fig. 9. First, the indicated envelope of the curves for the different T.S.-disturbance frequencies shifts considerably downstream in comparison with the incompressible situation shown in Fig. 6. At the same length-Reynolds number of 37.54×10^6 an n factor of 9 is reached at $x/L = 0.285$ at $M_\infty = 0.60$ in comparison to 0.22 for the incompressible condition. The point of neutral stability for the various frequencies is hardly affected by the increase in M_∞. Second, Fig. 9 shows that the most amplified disturbances in the range of $n = 9$ (at $x/L = 0.285$) have a frequency near 7,000 Hz, i.e., considerably higher than for the incompressible

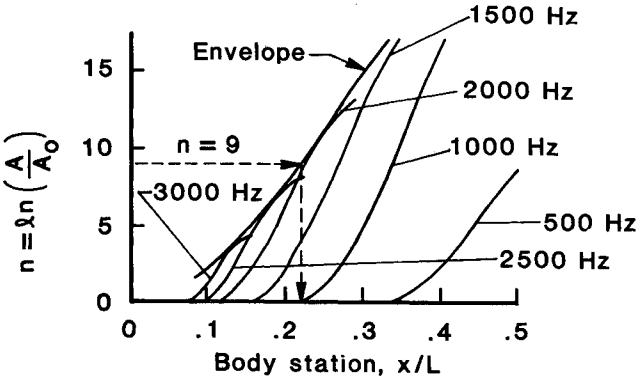

Fig. 6 Predicted incompressible T.S.-disturbance growth curves and frequency envelope over body 6.4-55; $\alpha = 0$ deg, $R_L = 37.54 \times 10^6$.

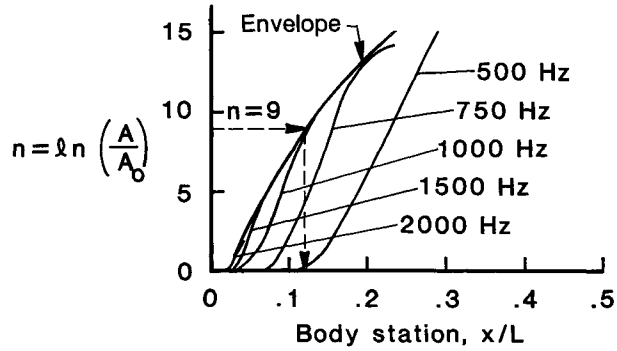

Fig. 7 Predicted incompressible T.S.-disturbance growth curves and frequency envelope over body 6.4-60; $\alpha = 0$ deg, $R_L = 40.0 \times 10^6$.

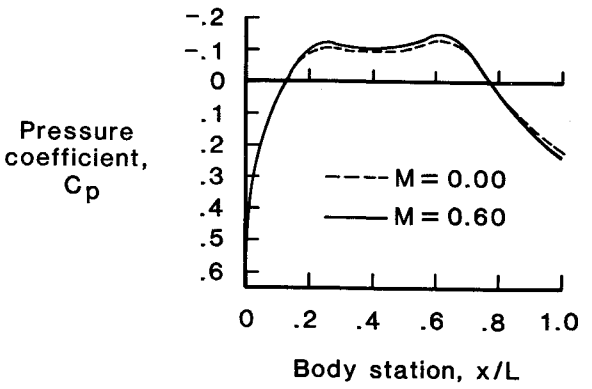

Fig. 8 Calculated pressure distributions over body 6.4-55 at incompressible speed and at $M_\infty = 0.60$, $\alpha = 0$ deg.

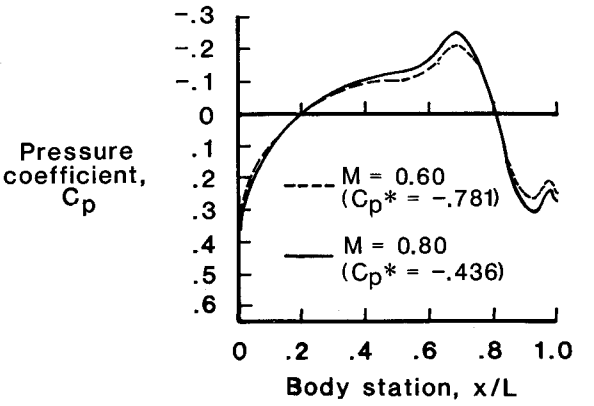

Fig. 11 Calculated compressible pressure distributions over body 6.4-60 at $M_\infty = 0.60$ and $M_\infty = 0.80$; $\alpha = 0$ deg.

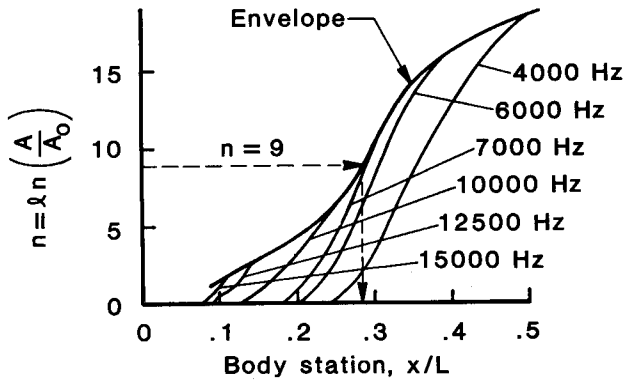

Fig. 9 Predicted compressible T.S.-disturbance growth curves and frequency envelope over body 6.4-55; $M_\infty = 0.60$, $\alpha = 0$ deg, $R_L = 37.54 \times 10^6$, $\psi = 0$ deg.

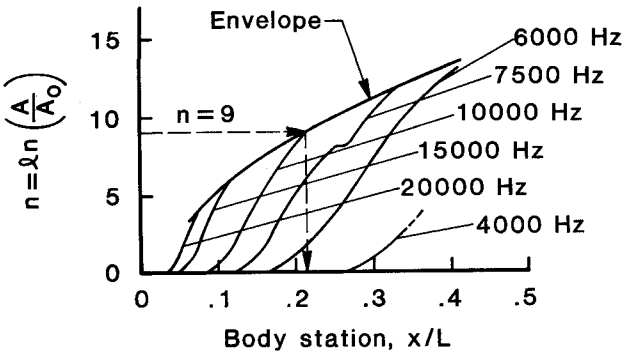

Fig. 12 Predicted compressible T.S.-disturbance growth curves and frequency envelope over body 6.4-60; $M_\infty = 0.60$, $\alpha = 0$ deg, $R_L = 40.0 \times 10^6$, $\psi = 0$ deg.

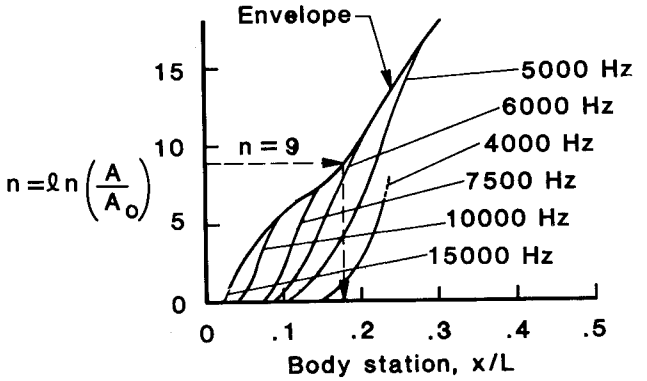

Fig. 10 Predicted compressible T.S.-disturbance growth curves and frequency envelope over body 6.4-55; $M_\infty = 0.60$, $\alpha = 0$ deg, $R_L = 86.6 \times 10^6$, $\psi = 0$ deg.

case. At $M_\infty = 0.60$, an n factor of 9 is reached downstream of the point of local minimum pressure at $x/L = 0.25$ for this body. Rapid growth in T.S. amplification occurs in the region of increasing pressure immediately downstream of the forebody minimum-pressure point. An example of the favorable effect of compressibility when increasing the length-Reynolds number is given in Fig. 10. This figure shows a COSAL analysis for the 6.4-55 fuselage at $M_\infty = 0.60$ at a length-Reynolds number of 86.6×10^6. Transition onset ($n = 9$) is predicted to occur at $x_{TR}/L = 0.18$ ($R_{TR} = 15.6 \times 10^6$) at $M_\infty = 0.60$ for this body. For the same body in incompressible flow, transition ($n = 9$) would occur near about $x/L = 0.22$ at $R_L = 37.54 \times 10^6$ (Fig. 7). In other words, for this geometry, an increase in freestream Mach number to 0.60 keeps the relative transition location almost unchanged near $x/L = 0.20$, although the length-Reynolds number has more than doubled.

Stability analyses at two subsonic Mach numbers were performed for the 6.4-60 body. Increasing the Mach number from near 0.0 to 0.60 results also for this body shape in a considerable increase in expected laminar run. Using the compressible pressure distribution given in Fig. 11, an amplification factor of 9 occurs near $x/L = 0.215$ (Fig. 12) at approximately twice the transition-Reynolds number of the incompressible case, while the most amplifying frequencies increase to 10,000 Hz. A further increase in freestream Mach number to 0.80 results in an additional decrease in T.S. growth rates for this axisymmetric body at $R_L = 40.0 \times 10^6$ (Fig. 13). In this case, the transition location (assumed when $n = 9$ is attained) is near $x/L = 0.30$ and a further increase in critical T.S. frequencies to about 15,000 Hz in the region where $n = 9$ is attained can be observed. Hence, a near tripling of transition-Reynolds number resulting from the favorable effects of flow compressibility is predicted for this body shape. In comparison to the results obtained at the lower Mach numbers, the slope of the frequency-envelope curve has decreased substantially, particularly for n factors above 9. In fact, an n-factor of 11 is not found forward of $x/L = 0.40$ for this body. Thus, in Fig. 13, the moderate slope of the envelope curve indicates that the transition process might start downstream of $x/L = 0.30$ over this body at $M_\infty = 0.80$.

Table 1 Calculated transition location and drag reduction at incompressible and compressible speeds

Geometry	M_∞	R_L, 10^6	x_{TR}/L	Fig. no.	C_D	$(C_D-C_{D_{ref}})/C_{D_{ref}}$
6.4-55	0.00	37.54	0.05		0.0451	
Body	0.00	37.54	0.22	6	0.0401	0.11
	0.60	37.54	0.05		0.0459	
	0.60	37.54	0.285	9	0.0380	0.17
	0.60	86.6	0.05		0.0459	
	0.60	86.6	0.18	10	0.0374	0.07
6.4-60	0.00	40.0	0.05		0.0421	
Body	0.00	40.0	0.12	7	0.0416	0.02
	0.60	40.0	0.05		0.0453	
	0.60	40.0	0.215	12	0.0422	0.07
	0.80	40.0	0.05		0.0446	
	0.80	40.0	0.30	13	0.0338	0.24

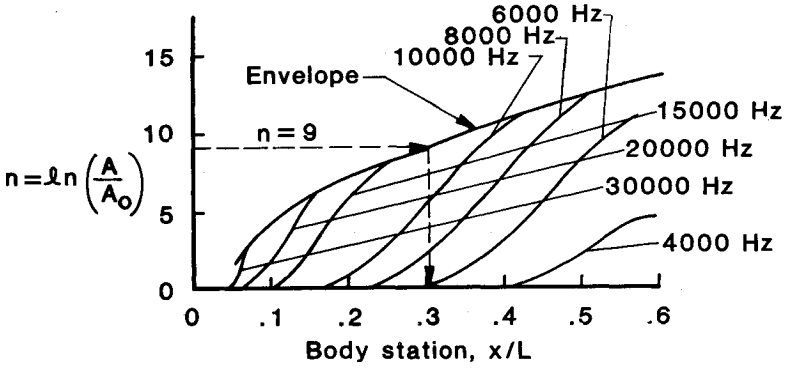

Fig. 13 Predicted compressible T.S.-disturbance growth curves and frequency envelope over body 6.4-60; $M_\infty = 0.80$, $\alpha = 0$ deg, $R_L = 40.0 \times 10^6$, $\psi = 0$ deg.

Drag Reduction Due to Compressibility Effect

To assess the impact of extending the length of laminar boundary-layer flow over the geometries analyzed in the compressible flow conditions, a calculation of the viscous drag is made using a modified integral boundary-layer approach.[8] An improved turbulent boundary-layer calculation method is incorporated in the panel method to give more realistic drag correlations with available experimental data. The turbulent boundary-layer calculations are based on Head's entrainment method as modified by Shanebrook and Sumner.[37] Validation of this improved method with experimental drag measurements by Gertler[38] on axisymmetric turbulent body shapes at R_L of 10.0×10^6 and 26.0×10^6 shows that the drag coefficient can be calculated very precisely for these predominantly turbulent-flow geometries.

Table 1 presents the drag calculated by this method for the body shapes of Figs. 4 and 5. The drag reduction obtained by moving the transition location from $x/L = 0.05$ to 0.22 in the incompressible flow case is estimated to be 11% for fuselage 6.4-55 at $R_L = 37.54 \times 10^6$. At $M_\infty = 0.60$, an additional 6% reduction in drag coefficient occurs when transition moves from $x/L = 0.22$ to 0.285 at the same length-Reynolds number, resulting in a total drag reduction of 17% in comparison to the reference body with $x_{TR}/L = 0.05$. Increasing the freestream Mach number to $M_\infty = 0.80$ for the 6.4-60 body results in a 24% decrease in drag when transition location moves from $x/L = 0.05$ to $x/L = 0.30$.

Concluding Remarks

Compressible linear boundary-layer stability analyses for two representative axisymmetric fuselage geometries predict a dominant favorable effect of compressibility on the stability characteristics of the axisymmetric laminar boundary layer at representative length-Reynolds numbers. Increasing the freestream Mach number from low subsonic to 0.60 and 0.80 significantly decreases T.S. growth rates in the laminar boundary layer on the bodies analyzed. Transition onset over a given fuselage shape with fineness ratio of 6.4 was predicted to move from 12% body length at incompressible speeds to more than 30% of the body length at $M_\infty = 0.80$ at a constant R_L of about 40×10^6, using the e^n-method. The almost tripled extent of laminar run is estimated to lead to a drag reduction of 24%. It is found that the generally destabilizing effect of increasing length Reynolds number on the stability of the laminar boundary layer can be overpowered by the favorable effect of compressibility of the fluid. At $M_\infty = 0.60$ the same amount of boundary-layer stability is realized at approximately twice the length-Reynolds number of the incompressible condition.

The favorable effect of compressibility might enable transition-Reynolds numbers of 20×10^6, which translates into a laminar boundary layer over half the length of a typical business-aircraft fuselage in cruise condition. Also, the predicted increase in laminar boundary-layer stability introduces a unique opportunity to maintain a natural laminar boundary layer over the forward portion of large transport fuselages. Provided the fuselage surface is sufficiently smooth, total transport-airplane drag reduction as high as 6% might be achieved with an NLF forebody. This favorable effect of compressibility also provides an opportunity to apply natural laminar flow over other near-axisymmetric airframe shapes, such as external fuel tanks and engine nacelles.

Acknowledgment

This research was supported by the NASA Langley Research Center under Grant NAG 1-345 to the University of Kansas,

Lawrence, Kansas, and Contract NAS1-17926 to Vigyan Research Associates, Inc., Hampton, Virginia.

References

[1]Holmes, B. J., Obara, C. J., and Yip, L., "Natural Laminar Flow Experiments on Modern Airplane Surfaces," NASA TP-2256, June 1984.

[2]Holmes, B. J., Obara, C. J., Martin, G. L., and Domack, C. S., "Manufacturing Tolerances for Natural Laminar Flow Airframe Surfaces," Society of Automotive Engineers Paper 850863, April 1985.

[3]Peterson, J. B. and Horton, E. A., "An Investigation of the Effect of a Highly Favorable Pressure Gradient on Boundary-Layer Transition as Caused by Various Types of Roughnesses on a 10-Foot-Diameter Hemisphere at Subsonic Speeds," NASA Memorandum 2-8-59L, April 1959.

[4]Althaus, D., "Wind-Tunnel Measurements on Bodies and Wing-Body Combinations," in *Motorless Flight Research, 1972*, NASA CR-2315, Nov. 1973.

[5]Radespiel, R., "Wind Tunnel Investigations of Glider Fuselages with Different Waisting and Wing Arrangements," NASA TM-77014, 1983.

[6]Hertel, H., *Structure-Form-Movement,* Reinhold, New York, 1966.

[7]Hertel, H., "Full Integration of VTOL Power Plants in the Aircraft Fuselage," *Gas Turbines,* AGARD Conference Proceedings No. 9, Part 1, 1966, pp. 69–96.

[8]Dodbele, S. S., Van Dam, C. P., Vijgen, P. M. H. W., and Holmes, B. J., "Shaping of Airplane Fuselages for Minimum Drag," *Journal of Aircraft,* Vol. 24, May 1987, pp. 298–304.

[9]Carmichael, B. H., "Underwater Drag Reduction Through Optimal Shape," *Underwater Missile Propulsion,* edited by L. Greiner, Compass Publications, Inc., Arlington, VA, 1966.

[10]Carmichael, B. H., "Application of Sailplane and Low-Drag Underwater Vehicle Technology to the Long-Endurance Drone Problem," AIAA Paper 74-1022, 1974.

[11]Carmichael, B. H., "Underwater Vehicle Drag Reduction Through Choice of Shape," AIAA Paper 66-657, June 1966.

[12]Parsons, J. S., Goodson, R. E., and Goldschmied, F. R., "Shaping of Axisymmetric Bodies for Minimum Drag in Incompressible Flow," *Journal of Hydronautics,* Vol. 8, July 1974, pp. 100–107.

[13]Dalton, C. and Zedan, M. F., "Design of Low Drag Axisymmetric Shapes by the Inverse Method," *Journal of Hydronautics,* Vol. 15, Jan.–Dec. 1981, pp. 48–54.

[14]Pinebrook, W. E. and Dalton, C., "Drag Minimization on a Body of Revolution Through Evolution," *Computer Methods in Applied Mechanics and Engineering,* Vol. 39, 1983, pp. 179–197.

[15]Dodbele, S. S., Van Dam, C. P., and Vijgen, P. M. H. W., "Design of Fuselage Shapes for Natural Laminar Flow," NASA CR-3970, March 1986.

[16]Boltz, F. W., Kenyon, G. C., and Allen, C. Q., "The Boundary-Layer Transition Characteristics of Two Bodies of Revolution, a Flat Plate, and an Unswept Wing in a Low-Turbulence Wind Tunnel," NASA TN-D-309, 1960.

[17]Groth, E. E., "Boundary-Layer Transition of Bodies of Revolution," Rept. No. NAI-57-1162, BLC-100, Northrop Aircraft Co., July 1957.

[18]Hefner, J. N. and Bushnell, D. M., "An Overview of Concepts for Aircraft Drag Reduction," *Special Course on Concepts for Drag Reduction,* AGARD Rept. 654, 1977.

[19]Quast, A. and Horstmann, K. H., "Profile Design for Wings and Propellers," NASA TM-77785, Nov. 1984.

[20]Georgyfalvy, D., "Effect of Pressurization on Airplane Fuselage Drag," *Journal of Aircraft,* Vol. 2, Nov.–Dec. 1965, pp. 531–537.

[21]Walsh, M. J. and Lindemann, A. M., "Optimization and Application of Riblets for Turbulent Drag Reduction," AIAA Paper 84-3468, 1984.

[22]Anders, J. B. and Watson, R. D., "Airfoil Large-Eddy Breakup Devices for Turbulent-Drag Reduction," AIAA Paper 85-0520, 1985.

[23]Runyan, J. L., Navran, B. H., and Rozendal, R. A., "F-111 Natural Laminar Flow Glove Flight Test Data Analysis and Boundary-Layer Stability Analysis," NASA CR-166051, Jan. 1984.

[24]Wentz, W. H. Jr., Ahmed, A., and Nyenhuis, R., "Natural Laminar Flow Experiments on a Swept-Wing Business Jet," AIAA Paper 84-2189, 1984.

[25]Holmes, B. J., Croom, C. C., Gall, P. D., Manuel, G. S., and Carraway, D. L., "Advanced Transition Measurements Methods for Flight Applications," AIAA Paper 86-9786, 1986.

[26]Mack, L. M., "Boundary-Layer Linear Stability Theory," *Special Course on Stability and Transition of Laminar Flow,* AGARD Rept. 709, 1984, pp. 3-1 to 3-81.

[27]Lees, L. and Lin, C. C., "Investigation of the Stability of the Laminar Boundary Layer in a Compressible Fluid," NACA TN-1115, Nov. 1944.

[28]Mack, L. M., "On the Stability of the Boundary Layer on a Transonic Swept Wing," AIAA Paper 79-0264, 1979.

[29]Maskew, B., "Prediction of Subsonic Aerodynamic Characteristics—A Case for Low-Order Panel Methods," *Journal of Aircraft,* Vol. 19, Feb. 1982, pp. 157–163.

[30]Harris, J. E. and Blanchard, D. K., "Computer Program for Solving Laminar, Transitional, or Turbulent Compressible Boundary-Layer Equations for Two-Dimensional and Axisymmetric Flow," NASA TM-83207, Feb. 1982.

[31]Malik, M. R., "Finite-Difference Solution of the Compressible Stability Eigenvalue Problem," NASA CR-3584, June 1982.

[32]Van Ingen, J. L., "A Suggested Semi-Empirical Method for the Calculation of the Boundary-Layer Transition Region," Technical University, Department of Aeronautics, Delft, Rept. VTH 74, 1956.

[33]Smith, A. M. O., "Transition, Pressure Gradients, and Stability Theory," *Proceedings of the 9th International Congress of Applied Mechanics,* Brussels, Vol. 4, 1956, pp. 234–244.

[34]Hefner, J. N. and Bushnell, D. M., "Status of Linear Boundary-Layer Stability Theory and the e^n Method, with Emphasis on Swept-Wing Applications," NASA TP-1645, Feb. 1980.

[35]Malik, M. R., "Instability and Transition in Supersonic Boundary Layers," *Laminar-Turbulent Boundary Layers, Proceedings of the Energy Sources Technology Conference,* New Orleans, LA, Feb. 1984, New York, 1984, pp. 139–147.

[36]Srokowski, A. J. and Orszag, S. A., "Mass Flow Requirements for LFC Wing Design," AIAA Paper 77-1222, 1977.

[37]Shanebrook, J. R. and Sumner, W. J., "Entrainment Theory for Axisymmetric, Turbulent Incompressible Boundary Layers," *Journal of Hydronautics,* Vol. 4, Oct. 1970.

[38]Gertler, M., "Resistance Experiments on a Systematic Series of Streamlined Bodies for Application to the Design of High-Speed Submarines," David Taylor Model Basin Rept. C-297, April 1950.